Pumps + Systems
Compressors, Compressed Air and Vacuum Technology

3rd International Rotating Equipment Conference (IREC)
Pumps, Compressors and Vacuum Technology
Düsseldorf, 14 – 15 September 2016

Influence of Surface Roughness on Cavitation in a Centrifugal Pump

Tim F. Groß, Gerhard Ludwig, Peter F. Pelz

Summary

Cavitation in centrifugal pumps is still a problem that must be dealt with by engineers and operators of such devices. Noise and vibration, erosion and limitations of the operating range ($NPSH_{3\%}$) are the most obvious consequences caused by cavitation. An efficient and reliable operation of centrifugal pumps is only possible if operators and designers have experience and knowledge about the different cavitation regimes that might occur and that differ in erosive potential and aggressiveness. The present paper shows how different surface roughnesses on the blades of the impeller influence the form of appearance of cavitation. Different cavitation regimes influence the NPSH curves and the corresponding $NPSH_{3\%}$ values only slightly even if appearance and size of the cavitation areas differ remarkably. The experiments also showed that cavitation and cavitation inception in centrifugal pumps is strongly affected by the occurrence of gap cavitation at the impeller side gap. Cavitation clouds produced at the gap are sucked into the pump and initiate cavitation at the leading edge of the blades. In this way large cavitation areas can develop even if the NPSH value is far away from the $NPSH_{3\%}$ limit.

VDMA
German Engineering Federation

Pumps + Systems
Chairman: Dr. Sönke Brodersen
Compressors, Compressed Air and Vacuum Technology
Chairman: Alexander W. Peters

Lyoner Str. 18
60528 Frankfurt am Main, Germany
Telefon +49 69 66 03-12 82
Telefax +49 69 66 03-22 82
E-Mail pu@vdma.org
Internet pu.vdma.org

VDMA
Technology Serving People

1. Introduction

The reliable and efficient operation of hydraulic machines such as pumps and turbines is feasible only in a limited working range. One limiting parameter is the occurrence of hydrodynamic cavitation. In the context of hydraulic machinery, the occurrence of cavitation is accompanied by several negative aspects. Cavitation influences the characteristic curves of the machines, is responsible for noise and vibration and causes damage of structural elements which is called cavitation erosion.

For engineers and operators dealing with cavitation in centrifugal pumps it is important to know that there are various kinds of cavitation regimes which differ in appearance, erosive potential and the region where they might occur. Failures of centrifugal pumps due to cavitation are often caused by a lack of knowledge about the different cavitation regimes and their aggressiveness. Therefore the prediction of critical operating parameters is of great value for system designers to identify harmful operation points already in the design process of such devices.

In centrifugal pumps one might observe single bubble cavitation, streak cavitation, sheet cavitation and cloud cavitation on the blades of the impeller. Vortex cavitation in shear layers, free jet cavitation at pressure relief bores and gap cavitation complete the picture of this complex phenomenon. In the present paper the focus is placed on the different cavitation regimes that occur on the blades of the impeller and how they are influenced by the surface roughness of the blades. In addition, the role of gap cavitation for the formation of cavitation on the blades is discussed.

The inception of cavitation on the blades usually coincides with the dynamic growth and collapse of so called nuclei that are either moving along freely with the liquid flow or are bounded to the surface at roughness elements. Nuclei are small amounts of gas (bubbles) that work as weak spots in the liquid and allow its rupture. The dynamic growth and collapse of these nuclei are a consequence of pressure changes in the liquid that occur due to high velocity gradients in the liquid flow. The numerous cavitation events can be distinguished from each other in time and space. Small-sized bubbles are usually spherical because of surface tension while sufficiently large bubbles show an elongated or in another manner deformed shape. The dynamics of spherical bubbles in an infinite liquid are described by the well-known Rayleigh–Plesset equation [1] [2]. Analytical and numerical considerations about cavitation noise and erosion usually rely upon the Rayleigh–Plesset equation (and its miscellaneous simplifications) and thus on single bubble cavitation.

Another observable cavitation regime is the large-scale sheet cavitation. In contrast to single bubble cavitation, a large area of the flow is either completely filled with vapor or appears as a bubbly mixture consisting of a huge number of small bubbles. Sheet cavitation evolves from single bubble cavitation if the local pressure is lowered either by a decreasing absolute pressure of the system or by an increasing flow velocity. Other common terms for sheet cavitation are fully developed cavitation and attached cavitation.

Yet another large-scale cavitation regime is transient cloud cavitation which usually evolves from sheet cavitation by further reducing the pressure. In contrast, this regime is characterized by the periodical formation, detachment and collapse of large vapor filled areas, so called clouds, observed by Knapp [3] for the first time. The detachment is either caused by the re-entrant jet that flows upstream beneath the sheet cavity [4] [5] or by shock waves as new studies show [6] [7] [8]. Franc [9] showed that the size of the detached clouds depends on the position the re-entrant jet breaks through the sheet cavity. Cloud cavitation is known for its erosive potential and as a source for extensive noise and vibrations. Therefore cloud cavitation is a primary cause of damages and functional limitations of hydraulic machines and components due to cavitation. The erosive potential of cloud cavitation has been studied by Pelz et al. [10]. A physical model describing the dynamics of cloud cavitation has been published by Buttenbender [11].

A further decrease of the pressure will lead to large cavitation structures that eventually cause a loss of pressure head. For the operation of pumps usually a head reduction of 3% is accepted. It is assumed that in this way damages due to cavitation erosion should be avoided. The 3% limit is not based on physical evidence but on experience. It is also linked to the $NPSH_{3\%}$ value of a pump which

defines the required conditions on the suction side of a pump and serves as a useful quantity for the design and dimensioning of pumps and pump systems.

In the present paper, we investigate the cavitation regimes occurring on the blades of a centrifugal pump depending on operation point and surface roughness by means of high-speed visualization. The paper is structured as follows. In section 2, we describe the experimental set-up and the experimental procedure. In section 3, the results of the experiments are presented and discussed. Section 4 closes the article with a conclusion.

2. Experimental set-up and experimental procedure

The centrifugal pump studied in this paper is part of the closed-loop test bench sketched in figure 1. The pump is powered by a speed controlled 90 kW electric motor. On the pressure side of the pump, a valve is used to adjust the volume flux and thus the incident flow on the impeller. To vary the absolute system pressure in a wide range from nearly 0 up to 3 bar a vacuum pump and a compressor are connected to an air vessel which is located on top of a tank. The tank is used as a water reservoir and furthermore allows bubbles to ascend so that they do not enter the suction pipe. We measure the volume flux by a magnetic-inductive flow meter (MID) that is positioned in the pressure pipe. Pressures are measured on the suction side and the pressure side of the pump. Furthermore, we measure the temperature and the oxygen content in the suction pipe. The last section of the suction pipe is made of acrylic glass to ensure a good optical accessibility. The high-speed visualizations are conducted with a 90° borescope (Karl Storz 88370DX) that is positioned in front of the impeller. By this means one achieves an undisturbed view on the impeller. With a Motion Pro Y7 S3 high-speed camera system we are enabled to record images with 10600 frames per second and a resolution of 1920 x 1080 pixels.

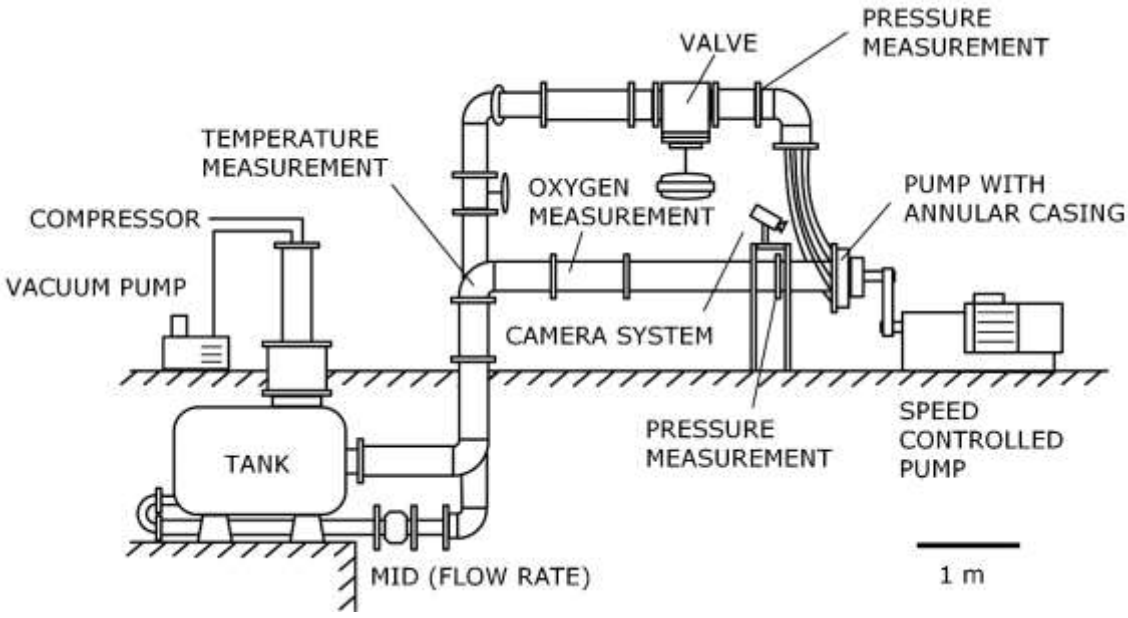

Figure 1: Sketch of the test rig

The investigated blades are screwed on the impeller and can be demounted to vary the surface roughness. Instead of a spiral casing we use an annular casing that is connected to the pipe with 12 tubes that are evenly distributed on the casing, see figure 2. By this means we achieve a uniform outflow condition and avoid disturbances of the flow due to the tongue of a spiral casing. Similar constructions have also been used in the extensive studies on cavitation in Braunschweig, e.g. [12] [13].

In our experiments we vary the roughness on the suction sides of the impeller blades and study how the cavitation regimes change. For varying the roughness, we apply a thin layer of glue and spread

small particles of silicon carbide over it. Figure 3 shows the different configurations that we surveyed. In all configurations with rough blades we used two different sizes of silicon carbide particles (152 µm and 52 µm). The configurations differ in the area that has been modified.

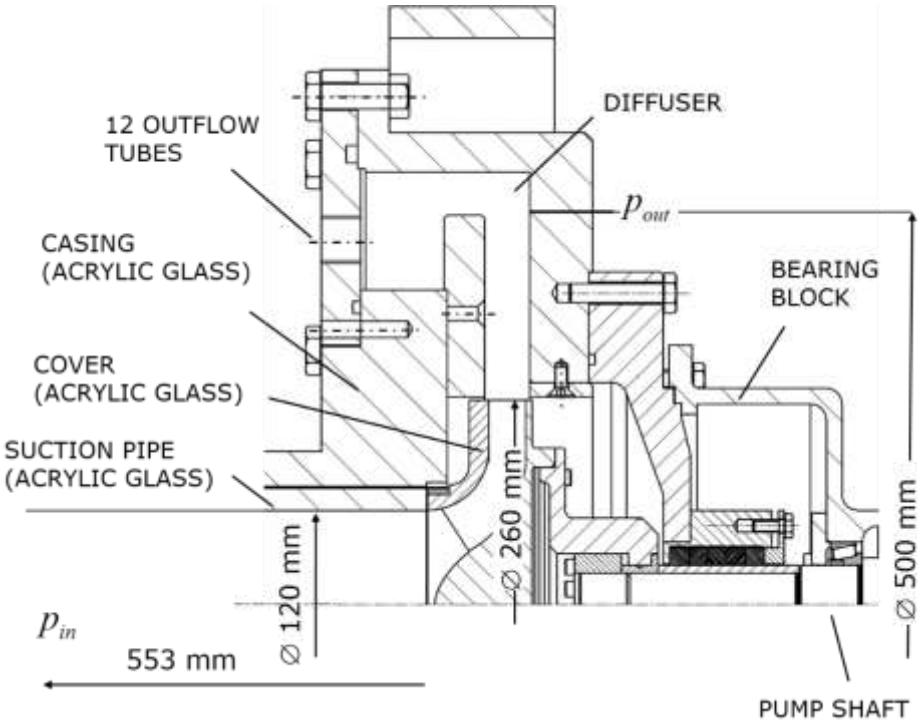

Figure 2: Section view of centrifugal pump.

Figure 3: Measured roughness configurations.

We investigate different operating points by varying the rotational speed of the pump and adjusting the flow rate with the valve in the pressure pipe. Furthermore, we change the absolute pressure in the system and thus the NPSH-value. In total, we recorded and analyzed more than 100 different configurations.

Pretests showed that the gas content – which is measured with an oxygen sensor – is a parameter that should not be ignored. The $NPSH_{3\%}$ value is highly affected by a high gas content in case of rough blades. In the experiments, the pressure is lowered to lower the NPSH value. This is linked to strong degassing processes. A huge amount of gas is released in the suction pipe and influences the cavitation occurrence and thus $NPSH_{3\%}$ significantly. In the experiments, we have ensured that the gas content is low to reduce the degassing processes to a minimum.

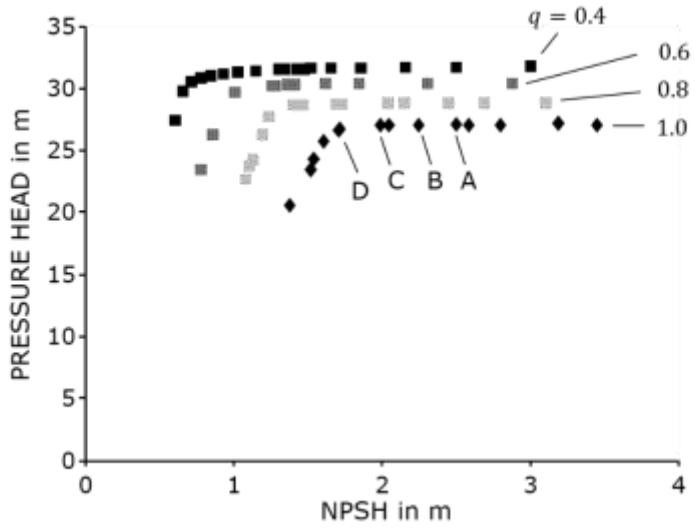

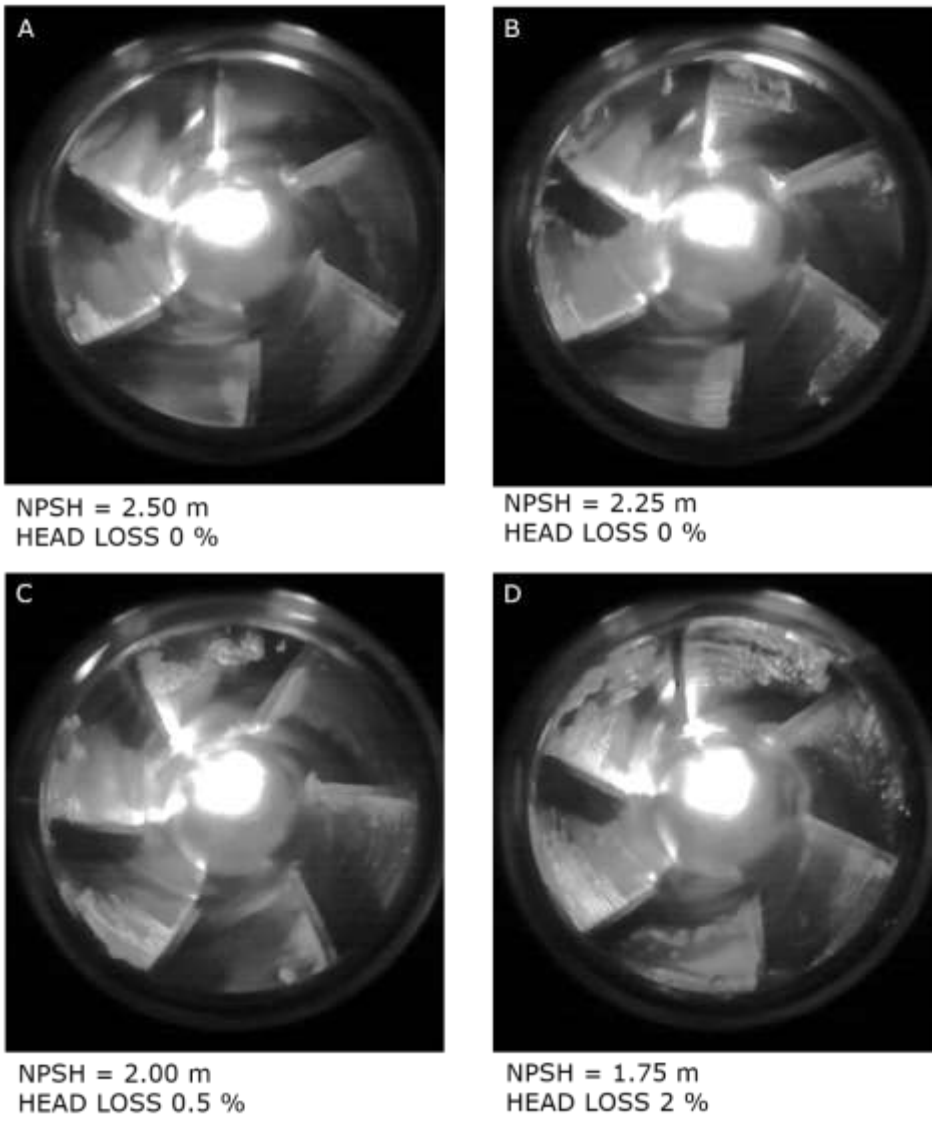

Figure 4: NPSH curve for different relative flow rates q = Q/Q_{opt}. (n = 1750 rpm) and four high-speed visualizations (exposure time 0.2 ms) of cavitation with q = 1.0 and different NPSH values, leading edge roughness 10 mm, k = 52 µm.

3. Experimental results and discussion

In the following section, we exemplarily show high-speed images that illustrate different phenomena we observed in our test rig. In order to correctly interpret the obtained results, the NPSH curve shown in figure 4 is useful. For better clarity, we only show high-speed visualizations for a rotational speed of 1750 rpm. Figure 4 also shows four high-speed images recorded at a constant relative flowrate $q = Q/Q_{opt} = 1.0$ with varying NPSH value. Here Q is the flow rate and Q_{opt} the flow rate in the design point at the given rotational speed. On the blades, a leading edge roughness (10 mm, k = 52 µm) is applied. For NPSH = 2.5 m (fig 4 A), only small cavitation areas occur. Not all of the six blades shows cavitation in this operating point. The cavitation areas on the blades can form and vanish in a short amount of time. While decreasing the NPSH value, the cavitation areas grow and most of the blades show cavitation nearly all of the time (B). The loss of pressure head (C) is usually accompanied by gap cavitation. A further decrease of the NPSH value leads to a significant decrease in pressure head (D) and the formation of large cavitation structures. The cavitation structures reach the blade channels which causes the observed loss of pressure head.

Figure 5: High-speed visualization (exposure time 0.2 ms) of impeller with different roughnesses (cf. figure 3) in the same operation point. q = 0.8, n = 1750 rpm, NPSH = 1.50 m.

Comparison of rough and smooth blades

Figure 5 exemplarily shows three high-speed images recorded in the test rig. The image on the left shows single bubble cavitation occurring on smooth blades. In case of a distributed roughness (k = 152 µm, images middle and right), the cavitation occurrence changes significantly. Instead of single bubbles that show a tremendous growth one observes sheet cavitation. The sheet cavity consists of a huge amount of small bubbles. The bubbles originate from the leading edge and move into the blade channels. In comparison to a completely rough blade, the blade with a leading edge roughness shows a more transient behavior at the tail of the sheet cavity. The described observations are illustrated in figure 6.

The classical image of a sheet cavity that rolls up and forms a cavitation cloud that has been observed in nozzles and on hydrofoils has not been observed in our experiments. The crucial part in the formation of a cloud is the formation of a re-entrant jet that flows upstream beneath the sheet cavity. The re-entrant jet can be interpreted as a thin viscous film which is driven by the stagnation pressure behind the sheet cavity, cf. [5]. In case of a completely rough blade the stagnation pressure is not big enough to overcome the losses so that the re-entrant is not streaming upstream very far. In case of a leading edge roughness the losses are way smaller because of the smooth surface in the area the re-entrant jet is moving. Nevertheless, we didn't observe cloud cavitation. This might be due to the complex flow situation in the pump. The sheet cavity might be disturbed by the main flow so that no larger sheet cavities can form. A second explanation is that even in the case with a leading edge roughness the stagnation pressure is too low. Thus, the re-entrant jet is only able to make a

small way upstream and peels off parts of the sheet cavity. This also explains why the tail of the sheet cavity shows a more transient behavior.

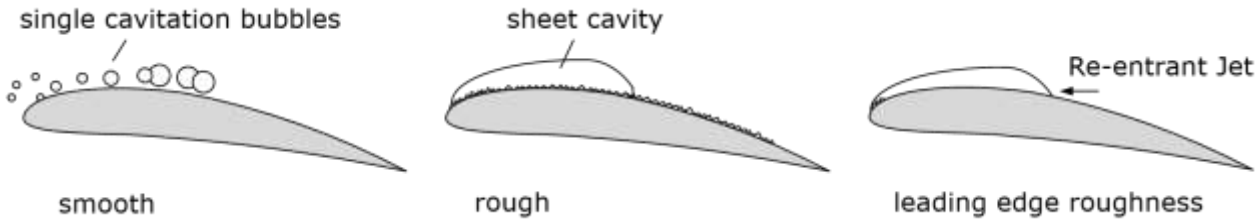

Figure 6: Sketch of cavitation regimes on blade in case of different roughnesses.

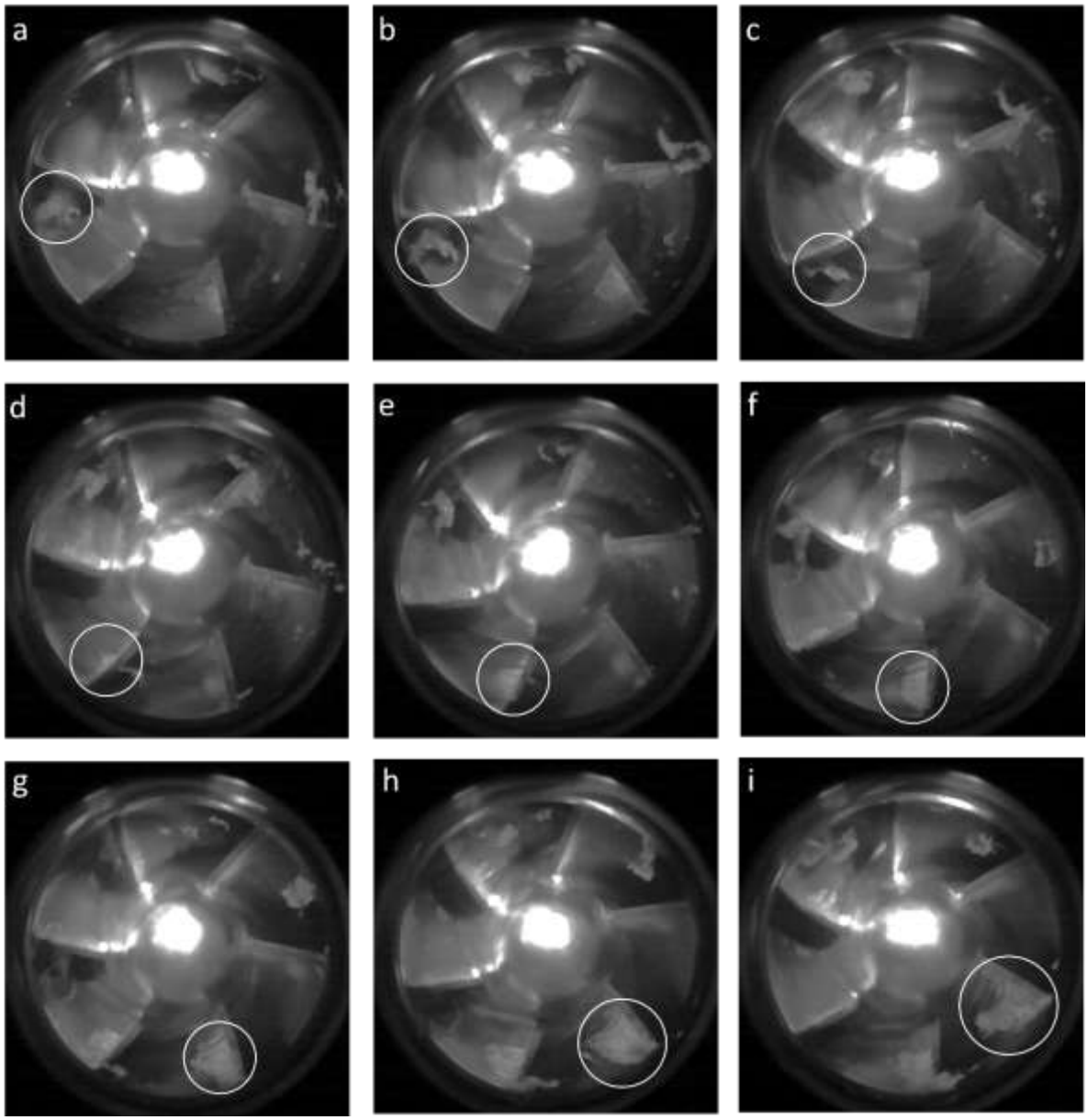

Figure 7: Formation of sheet cavitation due to gap cavitation. The time interval between the images is 2 ms. q = 0.4, n = 1750 rpm, NPSH = 2.50 m, rough leading edge 3 mm, k = 52 µm.

Influence of gap cavitation

The experiments also showed that the occurrence of cavitation on the blades is strongly affected by gap cavitation. Gap cavitation is capable of initiating cavitation on the blades. The blades cut through the cavitation structures that grow out of the gap and are sucked into the pump. Figure 7 illustrates this process. Image a, b and c show how a cavitating structure grows out of the gap. The moving blade (with leading edge roughness) comes closer to the structure and cuts through it (d) and a sheet cavity forms on the suction side of the blade (e). The sheet cavity expands radially and finally covers the complete leading edge of the blade (f-h). The sheet cavity expands and finally a part of it detaches as a cloud. As one can see, the other blades do not show large cavitation areas. With NPSH = 2.5 m, this operation point is far away from $NPSH_{3\%}$, cf. figure 4. It is remarkable that such big structures occur in such an operation point and shows that the $NPSH_{3\%}$ value is not a generally sufficient indicator for the occurrence of large cavitation phenomena and the erosive potential for every condition.

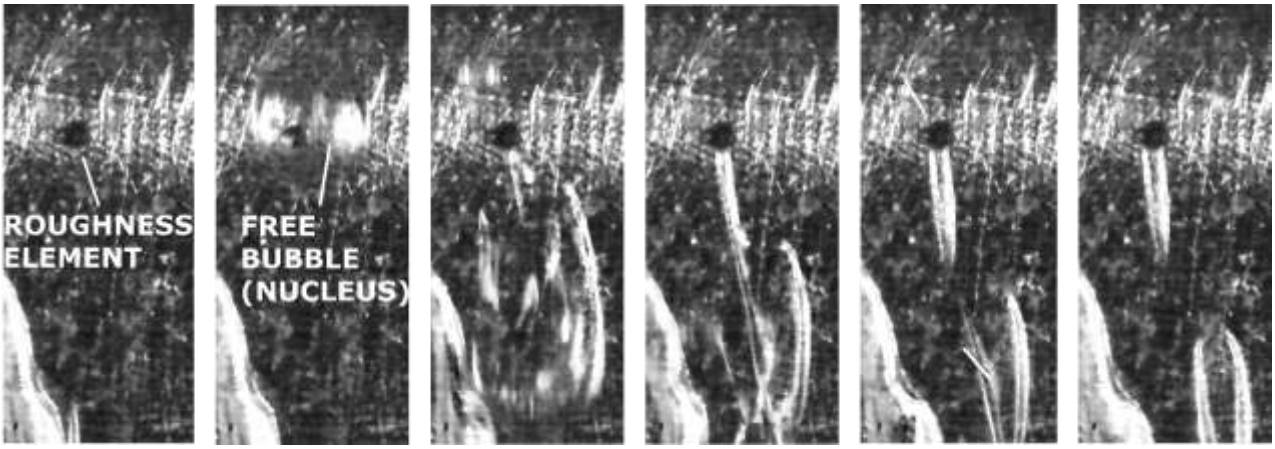

Figure 8: High-Speed visualization of the activation of a roughness element. The flow is from top to bottom. The time interval between the images is 0.2 ms. The roughness element has got a diameter of 0.1 to 0.15 mm.

From a scientific perspective the interaction of the cavitation structures with the rough surface is very challenging. The processes on the blades are not fully understood and unfortunately this topic is widely neglected in the cavitation community. The authors of this paper use generic experiments to investigate how free bubbles (e.g. originating from the gap cavitation) can activate roughness elements and how small amounts of gas in voids or crevices on surfaces influence degassing and the occurrence of cavitation [14] [15] [16]. Figure 8 exemplarily shows how a free bubble with a size of less than 1 mm interacts with a roughness element on a curved surface. Parts of the bubble are attached to the roughness element while the biggest part of the bubble passes by. The attached bubble grows due to gas diffusion and smaller bubbles detach. If many roughness elements are activated, see figure 9, large cavitation structures as seen in the centrifugal pump can occur.

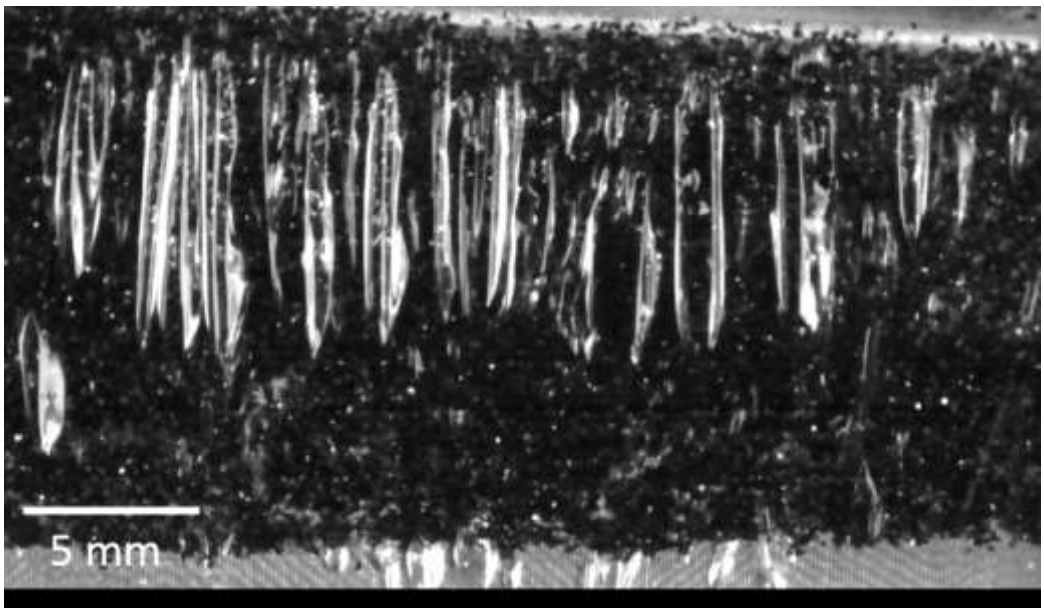

Figure 9: High-Speed visualization of the activation of a large amount of roughness element in a generic experiment. The flow is from top to bottom.

5. Conclusion

Cavitation in centrifugal pumps is still a problem that must be dealt with by engineers and operators of such devices. Noise and vibration, erosion and limitations of the operating range ($NPSH_{3\%}$) are the most obvious consequences caused by cavitation.

By means of high-speed visualization, new insights into the physics of cavitation in a centrifugal pump are presented. The experiments showed that the occurring cavitation regimes differ remarkably in their appearance depending on the surface roughness on the blades of the impeller. In case of smooth blades, one observes single bubble cavitation while rough blades lead to sheet cavitation in the same operation point. Applying a leading edge roughness intensifies the transient behavior of the sheet cavity.

A second issue that has been investigated is the role of gap cavitation for the formation of cavitation on the blades of the impeller. The experiments showed that gap cavitation can cause the formation of large cavitation structures on the blades when the blades move through cavitation structures that grow out of the gap. These cavitation structures consist of a huge amount of small bubbles that activate roughness elements on the surface of the blades.

Acknowledgement

The presented results were obtained within the research project No. 17482 N/1, funded by budget resources of the Bundesministerium für Wirtschaft und Technologie (BMWi) approved by the Arbeitsgemeinschaft industrieller Forschungsvereinigungen “Otto von Guericke” e.V. (AiF).

References

[1] M. S. Plesset, „The Dynamics of Cavitation Bubbles,“ *ASME J. Appl. Mech.,* Bd. 16, pp. 277-282, 1948.

[2] M. S. Plesset und A. Prosperetti, „Bubble Dynamics and Cavitation,“ *Ann. Rev. Fluid. Mech.,* Bd. 9, pp. 145-185, 1977.

[3] R. T. Knapp, „Recent Investigations of the Mechanics of Cavitation and Cavitation Damage," *Trans. ASME,* Bd. 77, pp. 1045-1054, 1955.

[4] P. Krishnaswamy, P. Andersen und S. A. Kinnas, „Re-Entrant Jet Modelling for Partially Cavitating Two-Dimensional Hydrofoils," in *Proceedings of CAV 2001: 4th International Symposium on Cavitation*, 2001.

[5] P. F. Pelz, T. Keil und T. F. Groß, „The transition from sheet to cloud cavitation," *under review in Journal of Fluid Mechanics,* 2016.

[6] S. L. Ceccio, „Mechanisms of Sheet to Cloud Transition for Partial Cavities," in *Key Note Lecture of CAV 2015: 9th International Symposium on Cavitation*, 2015.

[7] H. Ganesh, Bubbly Shock Propagation as a Cause of Sheet to Cloud Transition of Partial Cavitation and Stationary Cavitation Bubbles Forming on a Delta Wing Vortex, PhD-Thesis, The University of Michigan, 2015.

[8] C.-T. Hsiao, J. Ma und G. L. Chahine, „Multi-Scale Two-Phase Flow Modeling of Sheet and Cloud Cavitation," in *30th Symposium on Naval Hydrodynamics*, 2014.

[9] J.-P. Franc, „Partial Cavity Instabilities and Re-Entrant Jet," in *Proceedings of CAV 2001: 4th International Symposium on Cavitation*, 2001.

[10] P. F. Pelz, T. Keil und G. Ludwig, „Advanced Experimental and Numerical Techniques for Cavitation Erosion Prediction," K. Kim, G. Chahine, J. P-Franc und A. Karimi, Hrsg., Springer Netherlands, 2014.

[11] J. Buttenbender, Über die Dynamik von Kavitationswolken, Dissertation, Technische Universität Darmstadt: Shaker Verlag, 2012.

[12] V. Skara, J. Friedrichs und G. Kosyna, „Vortex Cavitation Occurring in Radial and Mixed flow Centrifugal Pump Impellers at Part-load Operation," *Proceedings of Pump Users International Forum 2012,* 2012.

[13] J. Friedrichs, Auswirkungen instationärer Kavitationsformen auf Förderhöhenabfall und Kennlinieninstabilität von Kreiselpumpen, Dissertation, TU Braunschweig, 2003.

[14] T. F. Groß, G. Ludwig und P. F. Pelz, „Experimental and theoretical investigation of nucleation from wall-bounded nuclei in a laminar flow," in *eingereicht bei: 16th International Symposium on Transport Phenomena and Dynamics of Rotating Machinery* , Honolulu, 2016.

[15] T. F. Groß, G. Ludwig und P. F. Pelz, „Experimental evidence of nucleation from wall-bounded nuclei in a laminar flow," in *9th International Symposium on Cavitation (CAV2015)*, Lausanne, 2015.

[16] T. F. Groß, G. Ludwig und P. F. Pelz, „High-Speed Visualisierung von Keimbildungsvorgängen an wandgebundenen Porenkeimen," in *Lasermethoden in der Strömungsmesstechnik GALA e.V.*, Dresden, 2015.